NANO LETTERS

2008
Vol. 8, No. 1
350−361

Smart Hydrogel Particles: Biomarker Harvesting: One-Step Affinity Purification, Size Exclusion, and Protection against Degradation

Alessandra Luchini,[†,‡] David H. Geho,[‡] Barney Bishop,[§] Duy Tran,[‡] Cassandra Xia,[‡] Robert L. Dufour,[‡] Clinton D. Jones,[‡,||] Virginia Espina,[‡] Alexis Patanarut,[§] Weidong Zhou,[‡] Mark M. Ross,[‡] Alessandra Tessitore,[‡] Emanuel F. Petricoin III,[‡] and Lance A. Liotta*[,‡]

CRO-IRCCS National Cancer Institute, Aviano, Italy, Center for Applied Proteomics and Molecular Medicine, George Mason University, Manassas, Virginia 20110, and Department of Chemistry and Biochemistry, George Mason University, Manassas, Virginia 20110

Received August 28, 2007; Revised Manuscript Received November 16, 2007

ABSTRACT

Disease-associated blood biomarkers exist in exceedingly low concentrations within complex mixtures of high-abundance proteins such as albumin. We have introduced an affinity bait molecule into *N*-isopropylacrylamide to produce a particle that will perform three independent functions within minutes, in one step, in solution: (a) molecular size sieving, (b) affinity capture of all solution-phase target molecules, and (c) complete protection of harvested proteins from enzymatic degradation. The captured analytes can be readily electroeluted for analysis.

There is an urgent need to discover novel biomarkers that provide sensitive and specific disease detection.[1,2] Cancer is rapidly becoming the leading cause of death for many population groups in the United States, largely because the disease is usually diagnosed after the cancer has metastasized, and treatment is ineffective. It is widely believed that early detection of cancer prior to metastasis will lead to a dramatic improvement in treatment outcome. Biomarkers are nucleic acids, proteins, protein fragments, or metabolites indicative of a specific biological state that are associated with the risk of the contraction or presence of disease.[3] Biomarker research has revealed that low-abundance circulating proteins and peptides present a rich source of information regarding the state of the organism as a whole.[4] Two major hurdles have prevented these discoveries from reaching clinical benefit: (1) disease-relevant biomarkers in blood or body fluids may exist in exceedingly low concentrations within a complex mixture of biomolecules and could be masked by high-abundance species such as albumin, and (2) degradation of protein biomarkers can occur immediately following the collection of blood or body fluid as a result of endogenous or exogenous proteinases. The goal of this study was to create "smart" nanoparticles that allow enrichment and encapsulation of selected classes of proteins and peptides from complex mixtures of biomolecules such as plasma, and protect them from degradation during subsequent sample handling. The captured analytes can be readily extracted from the particles by electrophoresis, allowing for subsequent quantitative analysis. This nanotechnology provides a powerful tool that is uniquely suited for the discovery of novel biomarkers for early-stage diseases such as cancer.

The concentration of proteins and peptides comprising the complex circulatory proteome ranges from 10^{-12} to 10^{-3} mg/mL, spanning 10 orders of magnitude, with a few high molecular weight proteins such as albumin and immunoglobulins accounting for 90% of total protein content.[5] However, the low-abundance and low molecular weight proteins and metabolites also present in the blood provide a wealth of information and have great promise as a source of new biomarkers. Conventional methods, such as two-dimensional (2-D) gel electrophoresis, do not have the sensitivity and resolution to detect and quantify low-abundance, low molecular weight proteins and metabolites. In spite of the moderately high sensitivity of modern mass spectrometers (attomolar concentration), their working range spans over

* Corresponding author.
† CRO-IRCCS National Cancer Institute.
‡ Center for Applied Proteomics and Molecular Medicine, George Mason University.
§ Department of Chemistry and Biochemistry, George Mason University.
|| Current address: Mercyhurst College.

10.1021/nl072174l CCC: $40.75
Published on Web 12/13/2007

3−4 orders of magnitude, and therefore the less abundant proteins are masked by more abundant proteins. Consequently, usual sample preparation steps for mass spectrometry (MS) experiments begin with the depletion of high abundant proteins using commercially available immunoaffinity depletion columns (Agilent, Sigma, and Beckman-Coulter). After depletion, fractionation is performed by means of size exclusion chromatography, ion exchange chromatography, and/or isoelectric focusing. However, removal of abundant native high molecular weight proteins can significantly reduce the yield of candidate biomarkers because it has been recently shown that the vast majority of low-abundance biomarkers are noncovalently and endogenously associated with the carrier proteins that are being removed.[6−9] Methods such as size exclusion ultrafiltration under denaturing conditions,[10] continuous elution denaturing electrophoresis,[11] or fractionation of serum by means of nanoporous substrates[12] have been proposed to solve this problem. Moreover, these same recent findings point to the low molecular weight region of the proteome as a rich and untapped source of biomarker candidates.[13−15]

In addition to the difficulties associated with the harvest and enrichment of candidate biomarkers from complex natural protein mixtures (such as blood), the stability of these potential biomarkers poses a challenge. Immediately following blood procurement (e.g., by venipuncture), proteins in the serum become susceptible to degradation by endogenous proteases or exogenous environmental proteases, such as proteases associated with the blood clotting process, enzymes shed from blood cells, or those associated with bacterial contaminants. Therefore, candidate diagnostic biomarkers in the blood may be subjected to degradation during transportation and storage. This becomes an even more important issue for the fidelity of biomarkers within large repositories of serum and body fluids that are collected from a variety of institutions and locations where samples may be shipped without freezing.

We evaluated the ability of hydrogel particles to perform directly, in one step and in solution, the size partition, affinity separation, concentration, and stabilization of low molecular weight proteins in serum as a new rapid method for blood-derived biomarker isolation and analysis. Hydrogels, by definition, are three-dimensional cross-linked polymeric networks that can imbibe large amounts of water.[16] They are usually formed through monomer polymerization in the presence of a cross-linking agent, which is typically a monomer with at least two polymerizable functional moieties. Gels can be categorized as nonresponsive (simple polymeric networks dramatically swell upon exposure to water) or responsive gels (have added functionality and display changes in solvation in response to certain stimuli such as temperature,[17] pH,[18,19] ionic strength,[20] light,[21,22] and electric field[23]). Poly(*N*-alkyl acrylamides) have been extensively studied with respect to their thermoresponsivity[16,24] with poly(*N*-isopropylacrylamide) (NIPAm) being one of the most strongly explored temperature-sensitive hydrogels within this group. NIPAm-containing particles are highly appealing for their potential biotechnological applications because of their stability, uniformity, and versatility with regard to the ease of making physical−chemical modifications in the particles. NIPAm particles have been investigated for drug delivery (slow release and targeted release) and for solute desorption,[25−36] interaction with cells,[26] and coupling with oligodeoxyribonucleotides as a solid phase for hybridization.[27] Since the size and porosity can be controlled by temperature, the use of temperature to control the targeted release of chemicals has been one of the most extensively characterized applications of NIPAm particles as vectors for controlled drug delivery.[28−34]

In the present study, hydrogel particles containing an affinity bait and a defined porosity were developed and demonstrated to (a) rapidly and in one step sequester the low molecular weight fraction of serum proteins, peptides, and metabolites, (b) remove and concentrate the target molecules from solution, and (c) protect captured proteins from enzymatic degradation.

NIPAm-based particles have been chosen because of their high water content, broad range of tunable porosities, consistency and uniformity following synthesis, functional reconstitution following freeze-drying, and potential biocompatibility. By changing the percentage of cross-linking agent and temperature, it is possible to control the particle size and the effective porosity. A significant advantage for the application studied here is the ability of these particles to rapidly uptake molecules because of their (a) open structure, (b) high water content, (c) dual hydrophobic and hydrophilic chemical moieties that can be substituted in the polymer, and (d) large surface area. This is a critical requirement for the goal of rapidly harvesting labile small proteins in solution and protecting the proteins from degradation. The small size, uniformity of particle dimension, and reproducibility from batch to batch of NIPAm provide a special advantage for applications in flow cytometry.

Hydrogel Particle Synthesis and Characterization. Gel particles incorporating *N*-isopropylacrylamide (NIPAm) were created and evaluated for molecular sieving properties. A second class of particles containing both NIPAm and acrylic acid (AAc), NIPAm/AAc,[16,18,35] was fabricated to incorporate a charge-based affinity bait into the particles. Particle synthesis chemistry is described in the Supporting Information.

Particle size dependence on temperature and pH were determined via photon correlation spectroscopy (submicron particle size analyzer, Beckman Coulter). Average values were calculated for three measurements using a 200 s integration time, and the solutions were allowed to thermally equilibrate for 10 min before each set of measurements. Measured values were then converted to particle sizes via the Stokes−Einstein relationship.[36] The NIPAm particle size decreased with increasing temperature (Figure 2A), which is a distinctive characteristic of thermoresponsive hydrogels.[28−33] The NIPAm/AAc particles showed a similar temperature dependence with respect to particle size; however, they also demonstrated a pH-dependent behavior (Figure 2B). At low pH (3.5), AAc groups are protonated, and the NIPAm/AAc particle size dependence on temperature is similar to that of

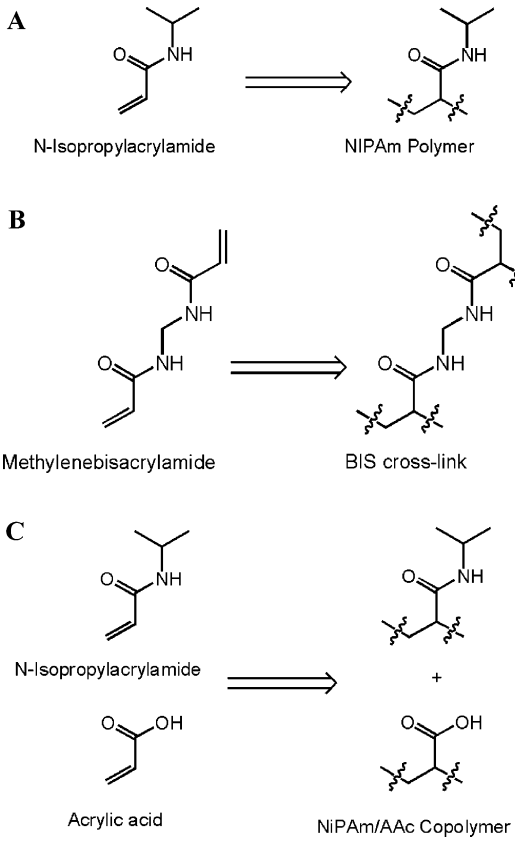

Figure 1. Chemical composition of particles. Structure of (A) NIPAm and its polymer, (B) methylenebisacrylamide, and (C) NIPAm and AAc and their polymers.

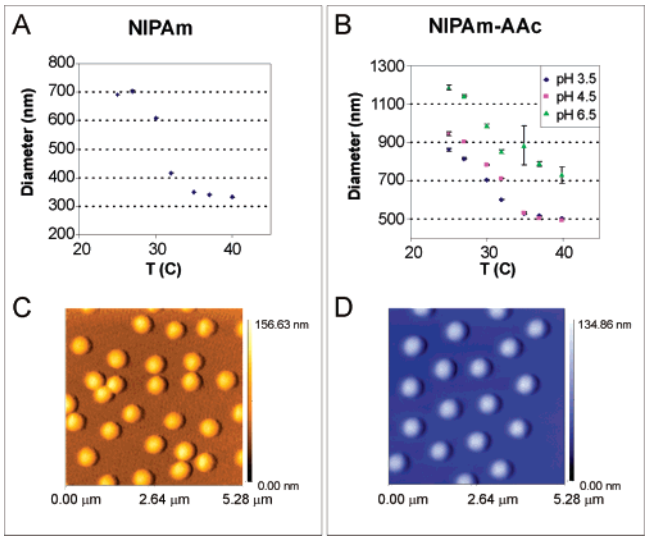

Figure 2. Particle characterization. (A) Light scattering measurement of NIPAm particle size as a function of temperature (diameter decreases as temperature increases). (B) Plots of correlation of the size of NIPAm/AAc particles with temperature (diameter decreases as temperature increases) and pH (diameter decreases as pH decreases). Also shown are AFM images of (C) NIPAm particles and (D) NIPAm/AAc particles on mica.

underivatized particles. At higher pH (4.5 and 6.5), AAc groups are partially deprotonated, and the average particle size increases, likely because of Coulombic interaction between polymeric chain and osmotic pressure resulting from counterion ingress in particles.[37,38]

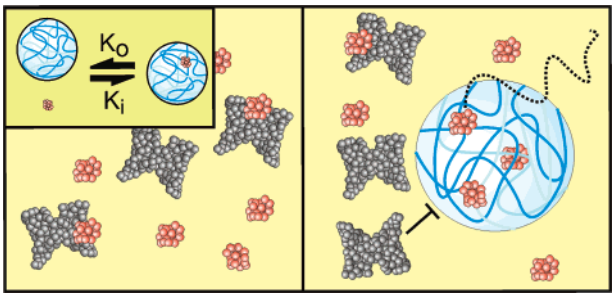

Figure 3. Schematic drawing of molecular sieving of particles in solution. Low molecular weight proteins are harvested; high molecular weight proteins are excluded.

Particles were further characterized by atomic force microscopy (AFM) using an NSCRIPTOR DPN System (NanoInk). Images were acquired under AC mode using a silicon tip with a typical resonance frequency of 300 kHz and a radius smaller than 10 nm. Aliquots of 1% w/v particles (50 μL) were deposited on freshly cleaved mica; samples were incubated for 10 min in humid atmosphere at room temperature to allow deposition, and then dried under nitrogen flow. AFM images of these particles (Figure 2C,D) show them to be homogeneous in size, with particle diameters consistent with those measured with light scattering.

Molecular Sieving by Hydrogel Particles. NIPAm particles were tested for their molecular sieve performance in solution, as schematically presented in Figure 3, the goal being to create particles that could capture proteins and small molecules with molecular weights less than approximately 20 000 Da since the peptidome is thought to contain a rich source of biomarkers.[13−15]

This size range contains informative proteins, peptides, and metabolites that are difficult, if not impossible, to separate from complex protein mixtures (such as serum or plasma) with adequate yield using 2-D gel electrophoresis or column chromatography. The chosen degree of cross-linking within the particle provided exclusion of albumin and other high-abundance large molecules while capturing molecules with sizes smaller than the cutoff pore size of the particles. Particles with varied degrees of cross-linking were investigated until one was identified that demonstrated an effective ~20 000 Da exclusive pore size. These particles were further studied in order to evaluate their sieving efficiency and nonspecific binding of excluded molecules to the particle surface. Because serum albumin is present in large excess (10^6-10^9-fold) relative to the proteins and peptides of interest, it was necessary to examine the efficiency and completeness of albumin exclusion.

Two independent methods were used to measure sieving performance: flow cytometry and gel electrophoresis. Aliquots of NIPAm particles (50 μL, 10 mg/mL) were incubated with target molecular species and centrifuged to collect the particles (7 min, 25 °C, 16 100 rcf). The supernatant was removed, and the particles were resuspended in 1 mL water. Centrifugation and washing were repeated three times, and the fluorescent intensity of the particles was measured using a FACScan flow cytometer (Becton Dickinson). The back-

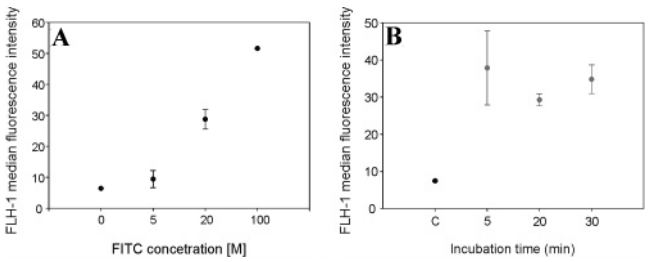

Figure 4. Flow cytometry analyses of FITC-incubated particles. (A) Uptake is dose dependent. (B) Uptake rapidly reaches saturation with FITC concentration of 20 μM.

ground fluorescent signal of untreated particles in water was used as a reference for all measurements. Fluorescein isothiocyanate (FITC, molecular weight (MW) 389 Da) was used as a model to study small molecule uptake and the dependence of uptake on incubation time and concentration. Particles incubated with various concentrations of FITC (5, 20, and 100 μM) showed a dose-dependent uptake rate (Figure 4A) toward saturation. Time course studies demonstrated that FITC uptake could occur rapidly (5 min, Figure 4B) at 10% v/v particle concentration.

NIPAm particles were also incubated with FITC-labeled bovine serum albumin (BSA), MW 66 000 Da, with a dye/molecule ratio of 1:1 (FITC−BSA, Sigma), FITC-labeled insulin, MW 3500 Da, with a dye/molecule ratio of 1:7 (Invitrogen), or FITC-labeled myoglobin, MW 17 000 Da, with a dye/molecule ratio of 1.36. Myoglobin (Sigma) was FITC-labeled by means of the HOOK−Dye Labeling Kit (G Bioscience) in accordance with the vendor's instructions. Concentrations of all fluorescent species were adjusted in order to equalize the fluorescence signal.

As shown in Figure 5A,B, particles incubated with FITC−BSA (MW 66 000 Da) have no detectable shift in fluorescence signal relative to the particle background fluorescence, which indicates no detectable BSA uptake or nonspecific binding by the particles. On the other hand, incubation with FITC−insulin (MW 3500 Da) results in a right shift in fluorescence relative to the control, confirming the uptake of insulin by the particles. FITC alone (MW 389 Da), a molecule in the size range of many metabolites, and FITC−myoglobin (MW 17 000 Da), another protein below the effective size cutoff of the particles, were both rapidly captured.

These findings were confirmed by sodium dodecyl sulfate polyacrylamide gel electrophoresis (SDS-PAGE) analysis. The particles were directly loaded on the gel after incubation with protein solution and washing. Insulin (Figure 5C), and myoglobin (Figure 5D) were trapped by particles, while BSA was totally excluded (Figure 5D).

Incorporation of a Charged Bait in the Molecular Sieving Particles Significantly Enhances Uptake. Passive molecular sieving cannot effectively harvest and concentrate all of the target proteins in solution because the concentration of the captured target protein in the particles is dependent on the equilibrium between rates of proteins exiting and entering particles and the concentration of the target protein in the bulk solution. Consequently, particles were constructed

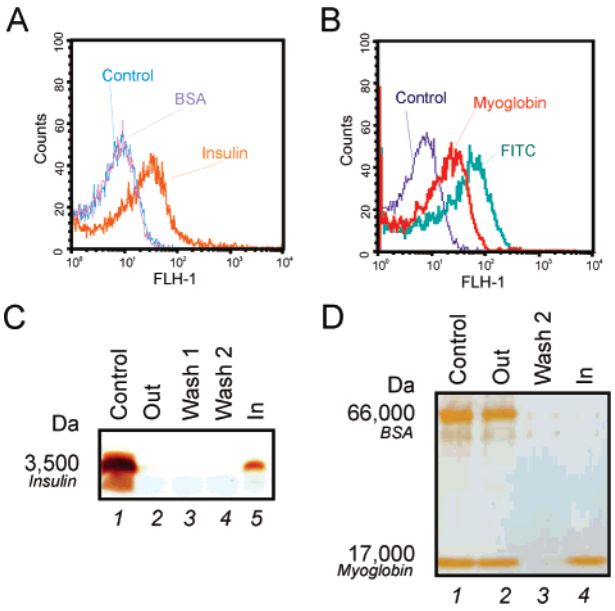

Figure 5. NIPAm particles incubated with FITC and FITC-labeled proteins: Flow cytometry measurements of (A) BSA and insulin, (B) myoglobin and free FITC. (C) SDS-PAGE of particles incubated with insulin: (1) insulin solution (Control); (2) NIPAm supernatant (Out, substance excluded from the particles); (3) wash 1; (4) wash 2; (5) NIPAm particles (In, substance captured by the particles). (D) SDS-PAGE of NIPAm particles incubated with BSA and myoglobin: (1) BSA and myoglobin (Control); (2) NIPAm supernatant (Out); (3) wash 2; (4) NIPAm particles (In). BSA is totally excluded.

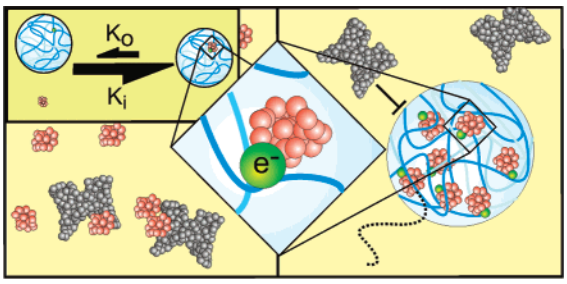

Figure 6. Schematic depiction of affinity-based sequestering.

that incorporated an affinity bait to facilitate harvesting of target proteins and prevent the captured proteins from exiting the particle.

A negatively charged moiety was selected as a bait for proteins and molecules that have a positive net charge. Incorporation of a negatively charged bait within the particles would allow the particles to preferentially sequester and concentrate positively charged proteins, peptides, and other biomolecules. Therefore, particles were prepared on the basis of a NIPAm/AAc copolymer, which carries a large net negative charge at pH values greater than 3.5. As shown schematically in Figure 6, the presence of charged bait, in principle, should substantially enhance the K_{eq} and thereby achieve a significantly higher concentration of the target protein inside the particle compared to the solution outside the particle.

As shown in Figure 7A, NIPAm/AAc particles concentrated analytes from solution with substantially greater

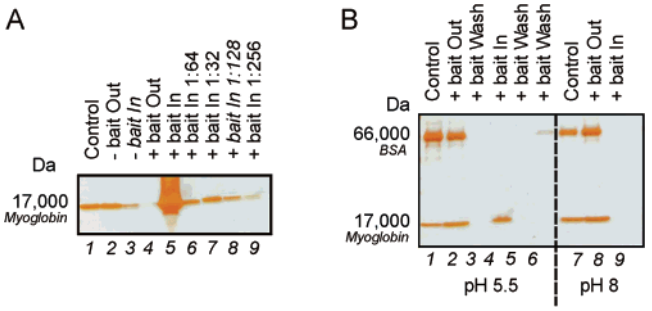

Figure 7. Protein sequestering by NIPAm/AAc particles (+ bait) versus NIPAm particles (− bait), SDS-PAGE analysis of (A) myoglobin (aqueous solution, pH 5.5) sequestration by particles + and − bait: (1) myoglobin; (2) NIPAm supernatant (Out); (3) NIPAm particle (In); (4) NIPAm/AAc supernatant (Out); (5) NIPAm/AAc particle (In); (6) NIPAm/AAc particles 1:64; (7) NIPAm/AAc particles 1:32; (8) NIPAm/AAc particles 1:128; and (9) NIPAm/AAc particles 1:256. (B) BSA and myoglobin sequestration by particles + bait (NIPAm/AAc) at two pH values. (1) BSA and myoglobin, pH 5.5; (2) NIPAm/AAc supernatant (Out), pH 5.5; (3) wash 3, pH 5.5; (4) NIPAm/AAc particles (In), pH 5.5; (5) wash 2, pH 5.5; (6) wash 1, pH 5.5; (7) BSA and myoglobin, pH 8; (8) NIPAm/AAc supernatant (Out), pH 8; and (9) NIPAm/AAc particles (In), pH 8.

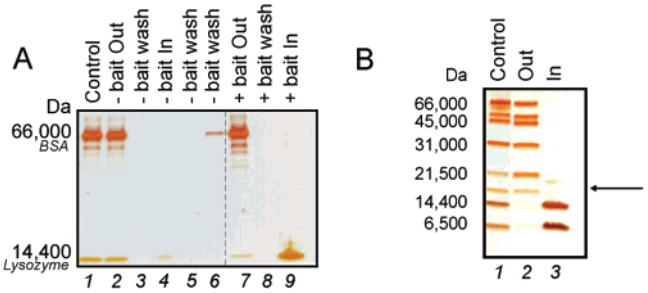

Figure 8. (A) SDS-PAGE analysis of particles − and + bait incubated with BSA and lysozyme: (1) BSA and lysozyme solution prior to particle introduction; (2) NIPAm (− bait) supernatant (Out); (3) wash 3; (4) NIPAm (− bait) particles (In); (5) wash 2; (6) wash 1; (7) NIPAm/AAc (+ bait) supernatant (Out); (8) wash 3; and (9) NIPAm/AAc (+ bait) particles (In). (B) SDS-PAGE analysis of NIPAm/AAc particles (+ bait) incubated with MW markers: (1) MW markers; (2) NIPAm/AAc supernatant (Out); and (3) NIPAm/AAc particles (In).

efficiency relative to underivatized NIPAm particles. Suspensions of NIPAm and NIPAm/AAc particles (10 mg/mL) were incubated for 1 h with myoglobin (MW 17 000 Da, 20 μM in water). Following incubation with NIPAm particles (without bait), significant levels of myoglobin remained in the bulk solution with some protein being bound by the particles, which lack the anionic affinity bait (Figure 7A). Following incubation with NIPAm/AAc particles, which contain the anionic affinity bait, all of the myoglobin had been captured by the NIPAm/AAc particles, with no detectable myoglobin remaining in bulk solution. Correlating myoglobin band intensity for serial dilutions of NIPAm/AAc particles with that of NIPAm particles suggests that the NIPAm/AAc particles sequestered myoglobin with more than 128-fold greater efficiency compared with particles that lack the affinity bait.

In order to demonstrate that the superior protein uptake associated with NIPAm/AAc particles was charge driven, aliquots of a solution containing myoglobin (20 μM) and BSA (20 μM) were incubated with NIPAm/AAc particles in phosphate buffer titrated to either pH 5.5 or pH 8 (Figure 7B). Particles were separated by centrifugation and washed three times with MilliQ water, as described above. At pH 5.5, myoglobin (pI 7) is expected to be positively charged, and electrostatic interactions between the protein and the negatively charged carboxyl groups of NIPAm/AAc particles would be attractive. However, at pH 8, myoglobin would be negatively charged, and any electrostatic interactions with the anionic particles would likely be repulsive in nature. Consistent with these expectations, myoglobin was efficiently sequestered by NIPAm/AAc particles at pH 5.5, where the protein and the particles have opposite net charges, and no myoglobin was detectable in particles that had been incubated with myoglobin at pH 8 (Figure 7B).

The efficiency of NIPAm/AAc affinity-baited particles to bind and concentrate proteins and peptides with MW less than ca. 20 000 Da is illustrated in Figure 8A. NIPAm/AAc and NIPAm particles were each incubated for 1 h with lysozyme (20 μM) and BSA (20 μM) in Tris (pH 7, 50 mM). The particles were then washed with three 1 mL volumes of water, and the captured proteins were electroeluted onto an SDS polyacrylamide gel.

While the NIPAm/AAc particles appeared to have captured all of the lysozyme present in the solution, there was no indication that BSA had been bound nonspecifically by the particles. As was observed with myoglobin, NIPAm particles, lacking the affinity bait, did not appear to significantly concentrate lysozyme.

A solution of protein molecular weight markers was used to further assess the molecular weight cutoff (MWCO) of the proteins sequestered by the particles (Figure 8B). The solution consisted of 0.5 mg/mL of each of the following proteins: aprotinin (MW 6500 Da, Sigma-Aldrich), lysozyme (MW 14 400 Da, Sigma-Aldrich), trypsin inhibitor (MW 21 500 Da, Invitrogen), carbonic anhydrase (MW 31 000 Da, Sigma-Aldrich), ovalbumin (MW 45 000 Da, Sigma-Aldrich), and BSA (MW 66 000 Da, Fisher Scientific) dissolved in Tris (pH 7, 50 mM). It was found that NIPAm/AAc-baited particles, incubated with the protein solution, effectively captured and concentrated all protein molecules with MW less than ca. 21 500 Da, and did not bind any proteins with MW greater than 21 500 Da. NIPAm particles showed a similar MWCO with MW $\leq$ 14 400 Da or smaller and not binding proteins MW $\geq$ 14 400 Da. The MWCO resolution achieved with NIPAm/AAc and NIPAm particles compares favorably with, or exceeds, that associated with standard molecular sieving chromatography.[39] In order to further indagate molecular sieving properties of the beads, NIPAm/AAc particles were incubated with platelet-derived growth factor B (PDGF B, 0.003 mg/mL, 14 500 Da, Cell Signaling) and BSA (0.067 mg/mL) in Tris (100 mM pH 7) for 1 h. The washing procedure was the same as described before. The SDS-PAGE in Figure 9 shows complete PDGF B uptake and BSA exclusion. PDGF B is a representative model for

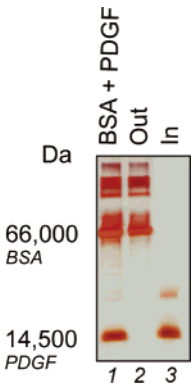

Figure 9. SDS-PAGE analysis of particles + bait incubated with PDGF B and BSA: (1) BSA and PDGF B; (2) NIPAm/AAc supernatant (Out); (3) NIPAm/AAc particles (In) (the faint upper band corresponds to dimerization of PDGF B after elution).

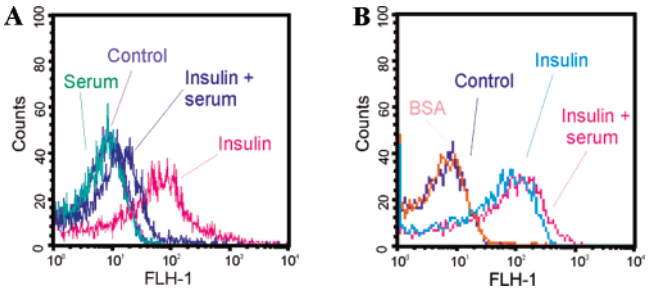

Figure 10. Flow cytometry analysis of (A) NIPAm and (B) NIPAm/AAc particles incubated with FITC-labeled insulin aqueous solution and FITC-labeled insulin spiked in serum, respectively.

a low-abundance, low molecular weight protein present in the blood, and PDGF B concentration in blood is 3.3 ng/mL.[40]

All the incubations presented in this study were conducted at room-temperature if not otherwise specified, since it is representative of real-world conditions. Nevertheless, because of the drastic change in size particles undergo when the temperature of solution is altered, temperature effects on MWCO were investigated. The solution of molecular weight markers described above was incubated with NIPAm/AAc particles at 4 and 40 °C, and the MWCO was approximately 10 000 Da higher at 4 °C with respect to 40 °C (data not shown).

On the basis of these results, we next tested the ability of the particles to capture small molecules spiked in complex solutions such as serum to mimic real-world biomarker discovery and analysis-type experiments. Aliquots of FITC-labeled insulin (final concentration 40 μM) in 1:10 diluted serum were incubated with NIPAm and NIPAm/AAc particles. Flow cytometry analysis demonstrated that NIPAm particles incubated in serum containing FITC−insulin yielded a right shift in fluorescence intensity relative to control particles and particles incubated with serum alone (Figure 10A).

This result clearly demonstrated the ability of NIPAm particles to capture insulin from a complex matrix such as serum. However, the capture efficiency of the NIPAm particles incubated with a simple aqueous solution containing

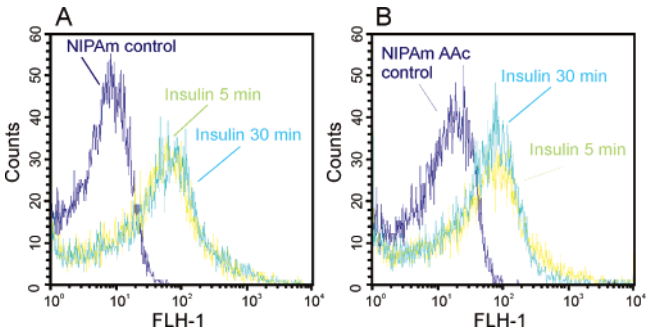

Figure 11. Flow cytometry time course studies of (A) NIPAm and (B) NIPAm/AAc particles incubated with FITC-labeled insulin.

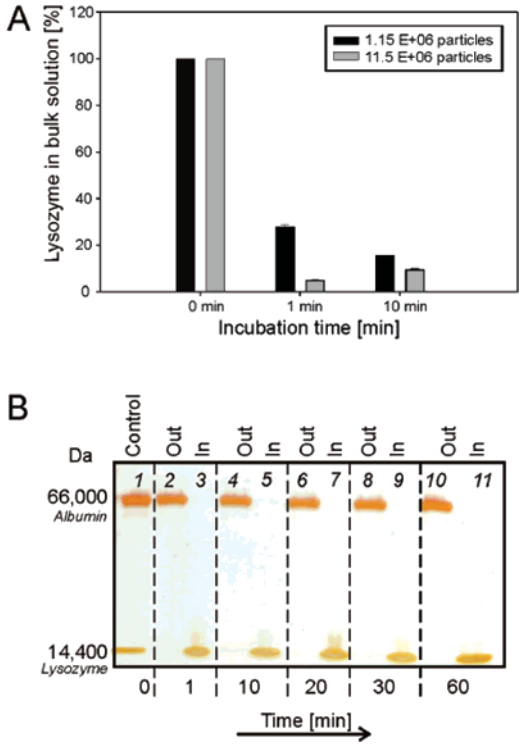

Figure 12. Uptake time course study. (A) Mean values of the percentage, relative to the initial amount, of lysozyme in solution incubated with two quantities of NIPAm/AAc particles as measured by RPPA (three replicate analyses and standard deviation shown). (B) SDS-PAGE analysis of a lysozyme and BSA solution incubated with NIPAm/AAc particles. Lane 1 is BSA and lysozyme solution. Lanes 2−11 are alternating supernatant (Out) and particles (In) for each of 5, 10, 20, 30, and 60 min incubation times. Lysozyme uptake is rapid and complete, while BSA exclusion is total.

only insulin was higher than that attained with serum-incubated NIPAm particles. While the two classes of particles exhibited a similar uptake of insulin in an aqueous solution, the particles with the charged bait were more efficient in capturing insulin spiked into serum compared to the underivatized particles. (Figure 10B).

Time course uptake studies for NIPAm and NIPAm/AAc particles incubated with FITC-labeled insulin (pI 5.3) were conducted in order to confirm and extend the data obtained for the small molecule, FITC. Histograms of fluorescence intensity associated with flow cytometry analyses of NIPAm and NIPAm/AAc particles incubated with FITC-labeled insulin collected at different time intervals are reported in

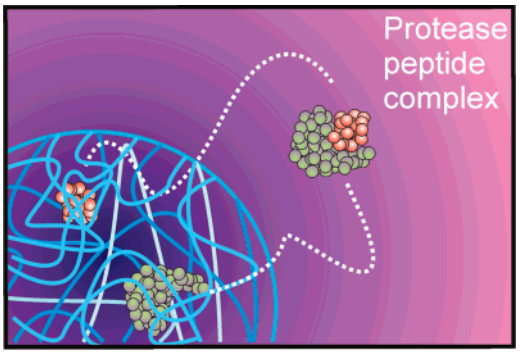

Figure 13. Schematic drawing illustrating the ability of particles to protect proteins from enzymatic degradation.

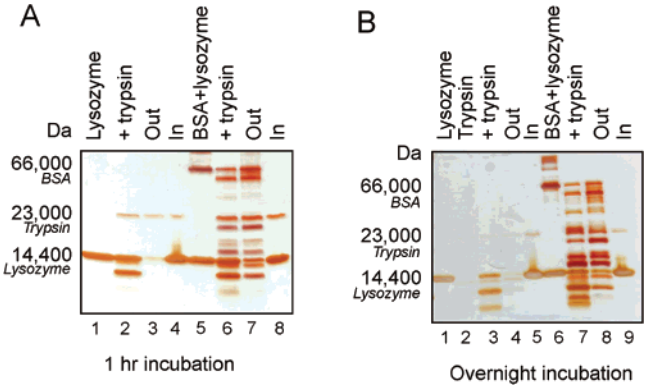

Figure 14. NIPAm/AAc particles (+ bait) protect bound proteins from degradation by enzymes that may be present. (A) NIPAm/AAc particles incubated with a solution containing lysozyme and trypsin for 1 h: (1) lysozyme; (2) lysozyme incubated with trypsin; (3) NIPAm/AAc supernatant (Out); (4) NIPAm/AAc particles (In); (5) BSA and lysozyme; (6) BSA and lysozyme + protease; (7) NIPAm/AAc particles supernatant (Out); and (8) NIPAm/AAc particles (In). (B) NIPAm/AAc particles incubated overnight with BSA, lysozyme, and trypsin: (1) lysozyme; (2) trypsin; (3) lysozyme + trypsin; (4) NIPAm/AAc supernatant (Out); (5) NIPAm/AAC particles (In); (6) lysozyme and BSA; (7) BSA and lysozyme + protease; (8) NIPAm/AAc supernatant (Out); and (9) NIPAm/AAc particles (In).

Figure 11. This data indicates that sequestration occurs rapidly (5 min) and is constant over time.

Rapid Time Course of Target Protein Uptake by Bait-Containing Particles. In order to prove that the kinetics of protein uptake is very rapid, the amount of protein remaining in bulk solution after incubation with NIPAm/AAc particles was measured by reverse-phase protein arrays (RPPA).[41] RPPA was chosen as a means to determine protein concentration in particle supernatant since it is a very sensitive quantitative technology (more sensitive by 3 orders of magnitude than other methods such as Bradford assays); our goal was to use a diluted protein solution in order to mimic the condition of low-abundance, low molecular weight proteins in the blood, and to evaluate the efficiency of complete protein removal from bulk solution. Different amounts of NIPAm/AAc particles (1.15 and 11.5 million) were incubated with lysozyme (20 μM) in Tris (pH 7, 50 mM) in a total volume of 100 μL for periods of 1 and 10 min. After centrifugation of the particles, aliquots of supernatant were spotted on a nitrocellulose-coated slide

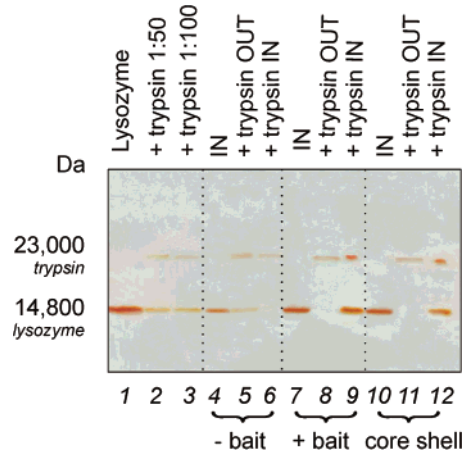

Figure 15. SDS-PAGE analysis of particles − bait, + bait, and core shell incubated with a solution containing reduced and alkylated lysozyme and trypsin: (1) reduced and alkylated lysozyme; (2) lysozyme + trypsin 1:50; (3) lysozyme + trypsin 1:100; (4) lysozyme with NIPAm particles (In); (5) lysozyme + trypsin + NIPAm particles supernatant (Out); (6) lysozyme + trypsin + NIPAm particles (In); (7) lysozyme + NIPAm/AAc particles (In); (8) lysozyme + trypsin + NIPAm/AAc particles supernatant (Out); (9) lysozyme + trypsin + NIPAm/AAc particles (In); (10) lysozyme + core shell (In); (11) lysozyme + trypsin + core shell particles supernatant (Out); (12) lysozyme + trypsin + core shell particles (In).

(FAST slide, Whatman) using an Aushon 2470 robotic arrayer (Aushon Biosystems). Arrays were stained with a colloidal gold solution, AuroDye Forte Kit (Amersham), images were acquired using a PowerLook 1120 scanner (Umax), and numeric values were obtained from images with ImageQuant (GE Healthcare) and processed with SigmaPlot (Systat). The bulk solution after a 1 min incubation with 1.15 million particles contained 28% of the initial protein amount, and 15% after 10 min. Moreover, the solution recovered from incubation with 11.5 million particles after 1 and 10 min contained 5% and 9% of the initial amount, respectively (Figure 12A). It should be noted that, since in all the time course experiments the separation of particles from solution was obtained by centrifugation, reported time values refer to incubation time intervals only. Beyond that, particles were in contact with solution for the additional 7 min required by centrifugation.

The kinetics of protein uptake by NIPAm/AAc particles was further investigated by incubating particles with BSA (20 μM) and lysozyme (20 μM) in Tris (pH 7, 50 mM) at room temperature and using SDS-PAGE to monitor lysozyme uptake at time points of 1, 10, 20, 30, and 60 min (Figure 12B). The results of this experiment showed that lysozyme sequestration was nearly complete after 1 min and was complete by 60 min, confirming that the process occurs very quickly as indicated in the flow cytometry time course study described above. As expected, BSA was excluded by the particles, and none of the BSA was taken up by the NIPAm/AAc throughout the duration of the experiment (60 min).

Demonstration of Isolation and Enrichment of Low Molecular Weight and Low-Abundance Analytes from Serum. The ability of NIPAM and NIPAm/AAc particles to sequester and concentrate low-concentration candidate

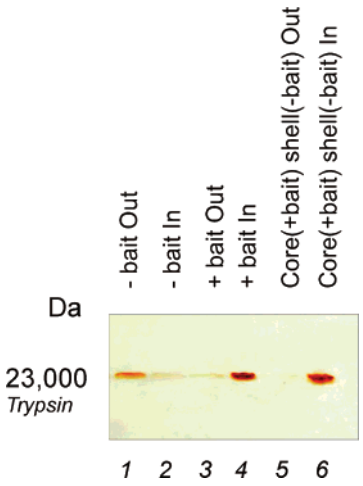

Figure 16. SDS-PAGE analysis of trypsin incubated with NIPAm, NIPAm/AAc, and core shell particles. Trypsin incubated with (1) − bait particles, supernatant (Out); (2) − bait particles (In); (3) + bait particles, supernatant (Out); (4) + bait particles (In); (5) core shell particles, supernatant (Out); (6) core shell particles (In).

protein biomarkers from serum for proteomic analysis was evaluated by incubating the particles with a 1:10 v/v dilution of serum in water for 1 h. The trapped proteins were electrophoretically eluted from the particles under denaturing conditions and then trypsin digested. The particles were heated in SDS sample buffer for 5 min at 100 °C and loaded on a 4−20% Tris Glicine gel (Invitrogen). Bands below approximately 30 kDa were cut, and in-gel trypsin digestion was performed.[11] The resulting peptide fragments were analyzed by online liquid chromatography/electrospray ionization tandem mass spectrometry (LC/ESI MS) using an LTQ-Orbitrap mass spectrometer (Thermo Fisher). A reverse-phase column was slurry-packed in-house with 5 μm, 20 Å pore size C18 resin (Michrom BioResources, CA) in 100 mm i.d. × 10 cm long fused silica capillary (Polymicro Technologies, Phoenix, AZ) with a laser-pulled tip. After sample injection, the column was washed for 5 min with mobile phase A (0.1% formic acid), and peptides were eluted using a linear gradient of 0% mobile phase B (0.1% formic acid, 80% acetonitrile) to 50% mobile phase B in 50 min at 200 nl/min, then to 100% B in an additional 5 min. The LTQ mass spectrometer was operated in a data-dependent mode in which each full MS scan was followed by five MS/MS scans, where the five most abundant molecular ions were dynamically selected and fragmented by collision-induced dissociation using a normalized collision energy of 35%. MS/MS data were matched against that of the NCBI (National Center for Biotechnology Information) human protein database with the program SEQUEST (Bioworks software, Thermo) using full tryptic cleavage constraints. High-confidence peptide identifications were obtained by applying the following filters to the search results: cross-correlation score (XCorr) ≥ 1.9 for 1+, 2.2 for 2+, 3.5 for 3+, and a maximum probability for a random identification of 0.01. The list of identified proteins (Tables 1 and 2 and Supporting Information) demonstrated that albumin and other high-abundance serum proteins were not present in the particles. Any protein presented must be a fragment of a larger parent protein if the native parent protein is above the MWCO. Thus abundant large-sized serum proteins can be represented as smaller sized low-abundance fragments. The specific nature of these fragments could have important diagnostic information. On the other hand, the list of identified proteins indicates that the particles sequestered rare and small-sized serum proteins and peptides.

Protein Sequestration by Particle Blocks Protease Degradation. One of the major problems associated with biological fluids is the potential for sample degradation during collection, transport, storage and analysis. Endogenous clotting cascade enzymes, enzymes released from damaged cells, or exogenous enzymes (from contaminating bacteria) can contribute to the degradation of diagnostically important proteins.

The lack of standardized preservation methods could result in bias in high-throughput analysis of serum and plasma.[42] While it was expected that proteases with MW greater than the MWCO of the particles (∼20 000 Da) would be excluded from the interior space of the particles and thereby be denied access to captured proteins, smaller proteases such as trypsin (23 800 Da) are more likely to be able to enter the particles. Additionally, it was not known whether proteases that entered charged-bait particles would retain their enzymatic potency when both the substrate proteins and the enzyme were sequestered by the particles (Figure 12). Therefore, NIPAm/AAc particles were incubated at 37 °C in a pH 7 NH_4HCO_3 (100 mM) solution containing lysozyme (0.5 mg/mL) and trypsin (0.05 mg/mL, Promega). Trypsin was selected for these studies because of its small size and the fact that the tryptic digestion of lysozyme would produce very characteristic cleavage products. The conditions used in this experiment would allow both lysozyme and trypsin to enter the particle. Analysis of the captured proteins by SDS-PAGE after incubation for 1 h and overnight showed only two bands—one corresponding to trypsin and the other corresponding to the full length lysozyme—indicating that no degradation of the protein had occurred (Figure 14A). Incubation of lysozyme (0.5 mg/mL) with trypsin (0.05 mg/mL) at 37 °C in a pH 7 NH_4HCO_3 (100 mM) solution in the absence of NIPAm/AAc particles resulted in the degradation of lysozyme. SDS-PAGE analysis of the reaction after incubation for 1 h and overnight clearly indicated the presence of low molecular weight peptide fragments, which showed that lysozyme was proteolyzed by trypsin in the absence of NIPAm/AAc particles. These results clearly indicate that sequestration of small proteins by affinity-bait particles can effectively shield bound proteins from proteases, including those that are capable of entering the particle interior.

In order to better understand the benefits associated with sequestration of proteins by NIPAm/AAc affinity-bait particles, NIPAm/AAc particles were incubated at 37 °C with a combination of BSA (0.5 mg/mL), lysozyme (0.5 mg/mL), and trypsin (0.05 mg/mL) in 100 mM NH_4HCO_3 (pH7).

As with the previous protection study, the reaction was analyzed using SDS-PAGE after incubating 1 h and overnight. In the absence of NIPAm/AAc particles, the majority

Table 1. MS Analysis of Proteins Electroeluted from NIPAm Particles after 1 h Incubation with 1:10 v/v Dilution Serum

reference	accession[a]	P_{pep}[b]	S_f[c]	score[d]	MW
complement component 1, q subcomponent, gamma polypeptide [*Homo sapiens*]	56786155.0	4.83E-12	3.43E+00	40.28	25757.13
complement component 1, r subcomponent [*Homo sapiens*]	66347875.0	5.65E-12	2.72E+00	30.24	80147.95
haptoglobin-related protein [*Homo sapiens*]	45580723.0	1.12E-11	9.76E-01	10.22	39004.70
PREDICTED: similar to Putative S100 calcium-binding protein A11 pseudogene [*Homo sapiens*]	113419208.0	1.12E-11	9.80E-01	10.22	11254.79
complement component 4A preproprotein [*Homo sapiens*]	67190748.0	1.12E-11	3.58E+00	40.24	192663.60
orosomucoid 1 precursor [*Homo sapiens*]	9257232.0	1.12E-11	8.17E-01	10.13	23496.77
CD5 antigen-like (scavenger receptor cysteine-rich family) [*Homo sapiens*]	5174411.0	1.12E-11	3.80E+00	40.25	38062.96
serum amyloid P component precursor [*Homo sapiens*]	4502133.0	1.12E-11	4.15E+00	50.20	25371.13
complement component 1, q subcomponent, B chain precursor [*Homo sapiens*]	87298828.0	1.12E-11	9.82E-01	10.26	26704.49
apolipoprotein A−I preproprotein [*Homo sapiens*]	4557321.0	1.12E-11	6.86E-01	10.12	30758.94
haptoglobin [*Homo sapiens*]	4826762.0	1.12E-11	3.70E+00	40.21	45176.59
complement component 1, q subcomponent, A chain precursor [*Homo sapiens*]	7705753.0	1.12E-11	8.24E-01	10.15	26000.19
platelet factor 4 (chemokine (C−X−C motif) ligand 4) [*Homo sapiens*]	4505733.0	1.12E-11	1.80E+00	20.16	10837.89
immunoglobulin J chain [*Homo sapiens*]	21489959.0	1.12E-11	9.45E-01	10.15	18087.00
lysozyme precursor [*Homo sapiens*]	4557894.0	1.12E-11	9.03E-01	10.15	16526.29
transthyretin [*Homo sapiens*]	4507725.0	1.12E-11	6.77E-01	10.13	15877.05
dermcidin preproprotein [*Homo sapiens*]	16751921.0	1.12E-11	8.66E-01	10.13	11276.83
mesotrypsin preproprotein [*Homo sapiens*]	21536452.0	1.12E-11	9.37E-01	10.17	26680.18
alpha 1 globin [*Homo sapiens*]	4504347.0	1.12E-11	9.62E-01	10.16	15247.92
beta globin [*Homo sapiens*]	4504349.0	1.12E-11	9.36E-01	10.17	15988.29
hypothetical protein LOC649897 [*Homo sapiens*]	91206438.0	1.12E-11	8.68E-01	10.18	22058.92
complement component 1, s subcomponent [*Homo sapiens*]	41393602.0	1.12E-11	9.25E-01	10.15	76634.85
protein kinase C and casein kinase substrate in neurons 2 [*Homo sapiens*]	6005826.0	1.12E-11	8.23E-01	10.15	55870.13
PREDICTED: similar to Keratin, type II cytoskeletal 2 oral (Cytokeratin-2P) (K2P) (CK 2P) [*Homo sapiens*]	89036176.0	1.12E-11	8.89E-01	10.14	36406.56
platelet factor 4 variant 1 [*Homo sapiens*]	4505735.0	1.12E-11	8.70E-01	10.19	11545.28
bromodomain containing 7 [*Homo sapiens*]	41350212.0	1.12E-11	8.63E-01	10.18	74092.27
SH3-domain binding protein 2 [*Homo sapiens*]	19923155.0	1.12E-11	2.64E-01	10.13	62220.29
zinc finger, CCHC domain containing 11 isoform c [*Homo sapiens*]	57863250.0	1.12E-11	8.14E-01	10.17	184587.10
apolipoprotein A-II preproprotein [*Homo sapiens*]	4502149.0	1.12E-11	8.90E-01	10.14	11167.90
heterogeneous nuclear ribonucleoprotein D isoform d [*Homo sapiens*]	51477708.0	1.12E-11	6.31E-01	10.18	30653.14
polo-like kinase 4 [*Homo sapiens*]	21361433.0	1.12E-11	6.16E-01	10.13	109016.40
apolipoprotein L1 isoform a precursor [*Homo sapiens*]	21735614.0	1.12E-11	6.63E-01	10.12	43946.95
coronin, actin binding protein, 2A [*Homo sapiens*]	16554583.0	1.12E-11	9.33E-01	20.14	59697.38

[a] "Accession" displays the unique protein identification number for the sequence. [b] "P_{pep}" displays the probability value for the peptide. [c] "S_f" displays the final score that indicates how good the protein match is. [d] "Score" displays a value that is based upon the probability that the peptide is a random match to the spectral data.

of BSA had been digested after 1 h, and the band corresponding to full-length BSA had disappeared after incubating overnight (Figure 14B). As was noted earlier, the NIPAm/AAC particles efficiently sequestered both lysozyme and trypsin and protected lysozyme from proteolysis by trypsin. However, the particles did not bind BSA, and the presence of low molecular weight bands in the supernatant after 1 h and overnight incubation accompanied by the decrease in intensity of the band corresponding to full-length BSA indicates that BSA was not protected from degradation by trypsin. Suppression of proteolytic activity by enzymes small enough to enter the particles, such as trypsin, may occur because immobilization of the enzymes by the charge-bait particle prevents them from binding substrate proteins or may be the result of steric hindrance associated with trapping of the substrate by the affinity-bait groups in the particle, thus preventing enzymes from productively binding target proteins inside the particle. Thus, the functional state of the proteins sequestered by the charge-bait may be similar to that of proteins arrested using a precipitating fixative treatment.

In order to exclude that nonspecific interactions of analytes exist with the surface charge of particles, we synthesized a batch of particles containing a NIPAm/AAc core covered by a NIPAm (non bait) shell (details on protocol available in the Supplemental Information). We then confirmed that core shell particles have the same sieving properties as NIPAm/AAc particles (Figure S1, Supporting Information).

Table 2. MS Analysis of Proteins Electroeluted from NIPAm/AAc Particles after 1 h Incubation with 1:10 v/v Dilution Serum

reference	accession[a]	P_{pep}[b]	S_f[c]	score[d]	MW
complement component 1, q subcomponent, gamma polypeptide [*Homo sapiens*]	56786155.0	3.55E-14	1.86E+00	20.30	25757.13
hypothetical protein LOC649897 [*Homo sapiens*]	91206438.0	3.55E-14	2.90E+00	30.26	22058.92
PREDICTED: similar to Putative S100 calcium-binding protein A11 pseudogene [*Homo sapiens*]	113419208.0	3.55E-14	1.46E+00	20.25	11254.79
apolipoprotein C−III precursor [*Homo sapiens*]	4557323.0	3.55E-14	9.79E-01	10.24	10845.50
pro-platelet basic protein precursor [*Homo sapiens*]	4505981.0	3.55E-14	5.61E+00	60.25	13885.42
complement component 3 precursor [*Homo sapiens*]	4557385.0	3.55E-14	9.80E-01	10.20	187045.30
small nuclear ribonucleoprotein polypeptide E [*Homo sapiens*]	4507129.0	3.55E-14	9.15E-01	10.19	10796.64
keratin 2 [*Homo sapiens*]	47132620.0	3.55E-14	5.75E+00	70.21	65393.19
albumin precursor [*Homo sapiens*]	4502027.0	3.55E-14	9.28E+00	100.22	69321.63
ribosomal protein L37a [*Homo sapiens*]	4506643.0	3.55E-14	9.73E-01	10.21	10268.48
complement component 4A preproprotein [*Homo sapiens*]	67190748.0	3.55E-14	1.91E+00	20.17	192663.60
A-gamma globin [*Homo sapiens*]	28302131.0	3.55E-14	9.44E-01	10.14	16118.27
platelet factor 4 (chemokine (C−X−C motif) ligand 4) [*Homo sapiens*]	4505733.0	3.55E-14	3.44E+00	40.18	10837.89
PREDICTED: hypothetical protein [*Homo sapiens*]	113418327.0	3.55E-14	8.55E-01	10.19	31688.42
H4 histone family, member J [*Homo sapiens*]	4504315.0	3.55E-14	1.51E+00	20.13	11360.38
lysozyme precursor [*Homo sapiens*]	4557894.0	3.55E-14	9.66E-01	10.20	16526.29
mesotrypsin preproprotein [*Homo sapiens*]	21536452.0	3.55E-14	9.68E-01	10.18	26680.18
alpha 1 globin [*Homo sapiens*]	4504347.0	3.55E-14	9.15E-01	10.14	15247.92
fibrinogen, alpha polypeptide isoform alpha-E preproprotein [*Homo sapiens*]	4503689.0	3.55E-14	8.35E-01	10.12	94914.27
hypothetical protein LOC55683 [*Homo sapiens*]	21361734.0	3.55E-14	6.53E-01	10.12	83244.77
crumbs homolog 1 precursor [*Homo sapiens*]	41327708.0	3.55E-14	6.87E-01	10.15	154080.40
PREDICTED: similar to glutamate receptor, ionotropic, N-methyl D-aspartate-like 1A isoform 1 isoform 1 [*Homo sapiens*]	41146739.0	3.55E-14	6.26E-01	10.15	41686.95
PREDICTED: similar to Neutrophil defensin 1 precursor (HNP-1) (HP-1) (HP1) (Defensin, alpha 1) [*Homo sapiens*]	113419903.0	3.55E-14	7.75E-01	10.12	10194.18
CDK5 regulatory subunit associated protein 1 isoform b [*Homo sapiens*]	28872784.0	3.55E-14	9.05E-01	10.12	56187.84
complement component 1, q subcomponent, B chain precursor [*Homo sapiens*]	87298828.0	3.55E-14	8.90E-01	10.15	26704.49
interferon-induced protein with tetratricopeptide repeats 3 [*Homo sapiens*]	31542980.0	3.55E-14	9.40E-01	10.22	55949.57
lamin A/C isoform 1 precursor [*Homo sapiens*]	27436946.0	3.55E-14	8.73E-01	10.14	74094.81
double *C*2-like domains, beta [*Homo sapiens*]	6005997.0	3.55E-14	5.53E-01	10.13	45920.53
desmoglein 4 [*Homo sapiens*]	29789445.0	3.55E-14	9.06E-01	10.13	113751.30
cadherin EGF LAG seven-pass G-type receptor 1 [*Homo sapiens*]	7656967.0	3.55E-14	1.56E+00	20.14	329276.70
procollagen, type III, alpha 1 [*Homo sapiens*]	4502951.0	3.55E-14	9.12E-01	10.15	138470.20
ATPase, H+ transporting, lysosomal 14kD, V1 subunit F [*Homo sapiens*]	20357547.0	3.55E-14	8.61E-01	10.16	13361.95

[a] "Accession" displays the unique protein identification number for the sequence. [b] "P_{pep}" displays the probability value for the peptide. [c] "S_f" displays the final score that indicates how good the protein match is. [d] "Score" displays a value that is based upon the probability that the peptide is a random match to the spectral data.

The use of lysozyme in its native form is a model mimicking the real-world physiological state and makes it possible to detect partial products of degradation with SDS-PAGE analysis. With this model it was proved that bait particles are able to protect the native protein from enzymatic degradation. Nevertheless, to verify how effective[43] is the protection from degradation of particles with bait, we used reduced and alkylated lysozyme denatured, and incubated it with trypsin and particles. Lysozyme was reduced by incubation with dithiothreitol (10 mM) in NH_4HCO_3 buffer (50 mM, pH 8) containing urea (2 M) for 1 h at room temperature. Iodoacetamide was added to the solution to a final concentration of 50 mM and allowed to react in the dark for 30 min. The lysozyme solution was diluted 1:2 with NH_4HCO_3 buffer (50 mM, pH 8) to a final concentration of 0.5 mg/mL. Aliquots of 50 μL of reduced and alkylated lysozyme were added to 50 μL of particles (10 mg/mL) in order to demonstrate that lysozyme by itself was captured by particles. In addition, trypsin was added to lysozyme solution at w/w ratios of 1:50 (0.01 mg/mL) and 1:100 (0.005 mg/mL). Particles with and without bait, and core shell particles were added to lysozyme−trypsin solution. All the

solutions were incubated for 1 h at 37 °C. Particles were washed as described above, and all samples were loaded on SDS-PAGE. In Figure 15 it is shown that (a) reduced and alkylated lysozyme undergoes trypsin-mediated proteolysis, and products of degradation are too small to be detected (lane 1−3); (b) lysozyme is captured by non-bait particles (lane 4), but in the presence of trypsin it is not protected from degradation, as is evident from the fact that the lysozyme band is absent in the particles (lane 6) and highly reduced in intensity in the supernatant (lane 5); (c) particles with bait harvest and concentrate denatured lysozyme (lane 7) and protect lysozyme from degradation (lane 9); and (d) likewise, core shell particles harvest, concentrate, and protect reduced and alkylated lysozyme from tryptic degradation. This suggests that the AAc bait plays a fundamental role in protecting proteins from degradation.

An incubation of trypsin (0.5 mg/mL in NH_4HCO_3 50 mM pH 8, 1 h, 37 °C) with particles was performed to corroborate the entrance of the enzyme in the beads. Trypsin is captured by plain particles, and is captured and concentrated by NIPAm/AAc and core shell particles (Figure 16).

We have described the development and application of hydrogel bait-containing particles as a new tool for harvesting and concentrating small molecule analytes and biomarker candidates from biological fluids, allowing high-throughput analysis of low-abundance and low molecular weight components. These nanoparticles present a rapid and straightforward workflow for direct utility in raw body fluids. While the work herein described particles with a negative charge that preferentially bind cationic species, positively charged particles such as a NIPAm/allylamine copolymer could be used to selectively harvest and concentrate anionic species from biological fluids. Similarly, hydrophobic metabolites could be captured for comprehensive metabolomic studies by using more hydrophobic particles such as NIPAm/styrene copolymers. Analyte-specific chemical or protein or nucleic acid affinity baits can be incorporated. For example, boronate-containing particles, which are known to bind saccharides, would be utilized to sequester glycoproteins from solution.[44] Consequently, NIPAm/allylamine copolymers are currently being synthesized that contain a bait for anionic proteins. Moreover, *p*-vinylphenylboronic acid is under consideration as a copolymer for harvesting sugars and nucleic acids. Further affinity baits such as triazinil-based reactive dyes (that have affinity toward proteins), hexadecylamine (for lipid uptake), and cyclodextrins (able to associate small molecules) are being noncovalently or covalently immobilized within the particles. In particular, we have used the bait chemistry described above to harvest the following small metabolites: L-DOPA, homogentisic acid, dopamine, DOPAC, and 5-hydroxyindoleacetic acid. This extends the utility of the technology to the realm of metabolomics.

Combining a variety of affinity chemistries with a size-sieving tool in a one-step process could have enormous utility for disease marker discovery and analysis workflows.

In the workflow presented in this study, proteins are denatured when eluted out of particles and then analyzed in MS for biomarker discovery. Nevertheless, it is important to note that the harvesting conditions are conducted with native protein mixtures. This permits future applications that require the analytes of interest to be in their native state (immunoassays, radioimmunoassays). For these applications, it would be important to maintain proteins in their native state when they are released from the particles. Using circular dichroism, Ahmad and colleagues demonstrated that molecules released from temperature-sensitive polymeric particles by temperature changes retained their native conformational state[45] Consequently, possible means of eluting native proteins from the particles include modifying the temperature or pH of the solution, increasing the ionic strength, or electroeluting the proteins under nondenaturing conditions.

Acknowledgment. The authors appreciate the generous support of Dr. Vikas Chandhoke and the Department of Life Sciences at George Mason University. The authors also thank Mr. Tom Huff for facilitating experimental procedures. We would like to acknowledge stimulating discussions with Dr. Enrico Garaci, Dr. Alfonso Colombatti, Dr. Claudio Belluco, Dr. Victor Morozov, and Dr. Michele Signore. This work was partly supported by the Italian Istituto Superiore di Sanità in the framework Italy/USA cooperation agreement between the U.S. Department of Health and Human Services, George Mason University, and the Italian Ministry of Public Health. This work was partially supported by the U.S. Department of Energy grant number 201270.

Supporting Information Available: Available in the Supporting Information are details on particle synthesis protocol, SDS-PAGE analysis on molecular sieving properties and enzymatic degradation, and tables (Table S1 and S2) listing proteins (with peptide coverage lists) identified via LC-MS/MS (ESI) on material electroeluted from NIPAm and NIPAm/AAc particles. This material is available free of charge via the Internet at http://pubs.acs.org.

References

(1) Aebersold, R.; Anderson, L.; Caprioli, R.; Druker, B.; Hartwell, L.; Smith, R. *J. Proteome Res.* **2005**, *4* (4), 1104−9.
(2) Srinivas, P. R.; Verma, M.; Zhao, Y.; Srivastava, S. *Clin. Chem.* **2002**, *48* (8), 1160−9.
(3) Frank, R.; Hargreaves, R. *Nat. Rev.* **2003**, *2* (7), 566−80.
(4) Espina, V.; Mehta, A. I.; Winters, M. E.; Calvert, V.; Wulfkuhle, J.; Petricoin, E. F., III; Liotta, L. A. *Proteomics* **2003**, *3* (11), 2091−100.
(5) Anderson, N. L.; Anderson, N. G. *Mol. Cell. Proteomics* **2002**, *1* (11), 845−67.
(6) Lopez, M. F.; Mikulskis, A.; Kuzdzal, S.; Golenko, E.; Petricoin, E. F., III; Liotta, L. A.; Patton, W. F.; Whiteley, G. R.; Rosenblatt, K.; Gurnani, P.; Nandi, A.; Neill, S.; Cullen, S.; O'Gorman, M.; Sarracino, D.; Lynch, C.; Johnson, A.; McKenzie, W.; Fishman, D. *Clin. Chem.* **2007**, *53* (6), 1067−74.
(7) Conrads, T. P.; Hood, B. L.; Veenstra, T. D. *BioTechniques* **2006**, *40* (6), 799−805.
(8) Lowenthal, M. S.; Mehta, A. I.; Frogale, K.; Bandle, R. W.; Araujo, R. P.; Hood, B. L.; Veenstra, T. D.; Conrads, T. P.; Goldsmith, P.; Fishman, D.; Petricoin, E. F., III; Liotta, L. A. *Clin. Chem.* **2005**, *51* (10), 1933−45.

(9) Lopez, M. F.; Mikulskis, A.; Kuzdzal, S.; Bennett, D. A.; Kelly, J.; Golenko, E.; DiCesare, J.; Denoyer, E.; Patton, W. F.; Ediger, R.; Sapp, L.; Ziegert, T.; Lynch, C.; Kramer, S.; Whiteley, G. R.; Wall, M. R.; Mannion, D. P.; Della Cioppa, G.; Rakitan, J. S.; Wolfe, G. M. *Clin. Chem.* **2005**, *51* (10), 1946−54.
(10) Zolotarjova, N.; Martosella, J.; Nicol, G.; Bailey, J.; Boyes, B. E.; Barrett, W. C. *Proteomics* **2005**, *5* (13), 3304−13.
(11) Camerini, S.; Polci, M. L.; Liotta, L. A.; Petricoin, E. F.; Zhou, W. *Proteomics Clin. Appl.* **2007**, *1*, 176−84.
(12) Geho, D.; Cheng, M. M.; Killian, K.; Lowenthal, M.; Ross, S.; Frogale, K.; Nijdam, J.; Lahar, N.; Johann, D.; Herrmann, P.; Whiteley, G.; Ferrari, M.; Petricoin, E.; Liotta, L. *Bioconjugate Chem.* **2006**, *17* (3), 654−61.
(13) Tirumalai, R. S.; Chan, K. C.; Prieto, D. A.; Issaq, H. J.; Conrads, T. P.; Veenstra, T. D. *Mol. Cell. Proteomics* **2003**, *2* (10), 1096−103.
(14) Merrell, K.; Southwick, K.; Graves, S. W.; Esplin, M. S.; Lewis, N. E.; Thulin, C. D. *J. Biomol. Tech.* **2004**, *15* (4), 238−48.
(15) Orvisky, E.; Drake, S. K.; Martin, B. M.; Abdel-Hamid, M.; Ressom, H. W.; Varghese, R. S.; An, Y.; Saha, D.; Hortin, G. L.; Loffredo, C. A.; Goldman, R. *Proteomics* **2006**, *6* (9), 2895−902.
(16) Pelton, R. *Adv. Colloid Interface Sci.* **2000**, *85* (1), 1−33.
(17) Li, Y.; Tanaka, T. *J. Chem. Phys.* **1990**, *92* (2), 1365−71.
(18) Jones, C. D.; Lyon, L. A. *Macromolecules* **2000**, *33* (22), 8301−6.
(19) Moselhy, J.; Wu, X. Y.; Nicholov, R.; Kodaria, K. *J. Biomater. Sci., Polym. Ed.* **2000**, *11* (2), 123−47.
(20) Duracher, D.; Sauzedde, F.; Elaissari, A.; Perrin, A.; Pichot, C. *Colloid Polym. Sci.* **1998**, *276* (3), 219−31.
(21) Sershen, S. R.; Westcott, S. L.; Halas, N. J.; West, J. L.; *J. Biomed. Mater. Res.* **2000**, *51*, 293−8.
(22) Suzuki, A.; Tanaka, T. *Nature* **1990**, *346* (6282), 345−7.
(23) Tanaka, T.; Nishio, I.; Sun, S.-T.; Ueno-Nishio, S. *Science* **1982**, *218*, 467−9.
(24) Inomata, H.; Goto, S.; Saito, S. *Macromolecules* **1990**, *23*, 4887−8.
(25) Kawaguchi, H.; Fujimoto, K.; Mizuhara, Y. *Colloid Polym. Sci.* **1992**, *270* (1), 53−7.
(26) Achiha, K.; Ojima, R.; Kasuya, Y.; Fujimoto, K.; Kawaguchi, H. *Polym. Adv. Technol.* **1995**, *6* (7), 534−40.
(27) Delair, T.; Meunier, F.; Elaissari, A.; Charles, M.-H.; Pichot, C. *Colloids Surf., A: Physicochem. Eng. Aspects* **1999**, *153* (1−3), 341−53.
(28) Sparnacci, K.; Laus, M.; Tondelli, L.; Bernardi, C.; Magnani, L.; Corticelli, F.; Marchisio, M.; Ensoli, B.; Castaldello, A.; Caputo, A. *J. Biomater. Sci., Polym. Ed.* **2005**, *16* (12), 1557−74.
(29) Hiratani, H.; Mizutani, Y.; Alvarez-Lorenzo, C. *Macromol. Biosci.* **2005**, *5* (8), 728−33.
(30) Nahar, M.; Dutta, T.; Murugesan, S.; Asthana, A.; Mishra, D.; Rajkumar, V.; Tare, M.; Saraf, S.; Jain, N. K. *Crit. Rev. Ther. Drug Carrier Syst.* **2006**, *23* (4), 259−318.
(31) Wu, J.-Y.; Liu, S.-Q.; Heng, P. W.-S.; Yang, Y.-Y. *J. Controlled Release* **2005**, *102* (2), 361−72.
(32) Zhang, X. Z.; Lewis, P. J.; Chu, C. C. *Biomaterials* **2005**, *26* (16), 3299−309.
(33) Woo, B. H.; Jiang, G.; Jo, Y. W.; DeLuca, P. P. *Pharm. Res.* **2001**, *18* (11), 1600−6.
(34) Basinska, T. *Macromol. Biosci.* **2005**, *5* (12), 1145−68.
(35) Saunders, B. R.; Vincent, B. *Adv. Colloid Interface Sci.* **1999**, *80* (1), 1−25.
(36) Pecora, R. *Dynamic Light Scattering: Applications of Photo Correlation Spectroscopy*; Planum Press: New York, 1985; p 436.
(37) Fernandez-Nieves, A.; Fernandez-Barbero, A.; Vincent, B.; de las Nieves, F. J. *Macromolecules* **2000**, *33*, 2114−8.
(38) Ito, S.; Ogawa, K.; Suzuki, H.; Wang, B.; Yoshida, R.; Kokufuta, E. *Langmuir* **1999**, *15* (12), 4289−94.
(39) Boschetti, E. *J. Chromatogr. A* **1994**, *658* (2), 207−36.
(40) Eppley, B. L.; Woodell, J. E.; Higgins, J. *Plast. Reconstr. Surg.* **2004**, *114* (6), 1502−8.
(41) Gulmann, C.; Sheehan, K. M.; Kay, E. W.; Liotta, L. A.; Petricoin, E. F., III. *J. Pathol.* **2006**, *208* (5), 595−606.
(42) Ayache, S.; Panelli, M.; Marincola, F. M.; Stroncek, D. F. *Am. J. Clin. Pathol.* **2006**, *126* (2), 174−84.
(43) Noda, Y.; Fujiwara, K.; Yamamoto, K.; Fukuno, T.; Segawa, S.-I. *Biopolymers* **1994**, *34* (2), 217−26.
(44) Ivanov, A. E.; Galaev, I. Y.; Mattiasson, B. *J. Mol. Recognit.* **2006**, *19* (4), 322−31.
(45) Ahmad, H.; Okubo, M.; Kamatari, Y. O.; Minami, H. *Colloid Polym. Sci.* **2002**, *280* (4), 310−315.

NL072174L